

Noise Characteristics and Particle Detection Limits in Diode+MTJ Matrix Elements for Biochip Applications

F. A. Cardoso^{1,2}, R. Ferreira^{1,2}, S. Cardoso^{1,2}, J. P. Conde^{1,2}, V. Chu¹, P. P. Freitas^{1,2}, J. Germano^{1,3}, T. Almeida^{1,3}, L. Sousa^{1,3}, and M. S. Piedade^{1,3}

¹Instituto Nacional de Engenharia de Sistemas e Computadores—Microsistemas e Nanotecnologias (INESC-MN), Lisbon 1000-029, Portugal

²Instituto Superior Tecnico (IST), Lisbon 1000-029, Portugal

³Instituto Nacional de Engenharia de Sistemas e Computadores—Investigação e Desenvolvimento (INESC-ID), Lisbon 1000-029, Portugal

A fully scalable matrix-based magnetoresistive biochip has been recently introduced for the detection of biomolecular recognition events. This work reports results for a 3×3 cells matrix comprising hydrogenated amorphous silicon diodes (PIN and Schottky) and aluminum oxide magnetic tunnel junctions (MTJ). The noise characteristics of the individual thin film diodes (TFD) and the MTJ were analyzed for measuring frequencies from DC to 1 kHz, allowing the detection of single magnetic nanoparticles with 250 nm and 130 nm diameters. For 50 nm particles, and at 1 kHz, minimum number of detectable labels ranges from 20 (Schottky diodes) to 50 (PIN diodes).

Index Terms—DNA-chips, magnetic nanoparticles, magnetic tunnel junction, magnetoresistive biochips.

I. INTRODUCTION

RECENTLY, fully integrated magnetoresistive (MR) sensor-based biochip platforms have been introduced for biomolecular recognition detection using magnetic labels [1]–[7]. In these assays, the labelled target biomolecules are subsequently recognized by biomolecular probes immobilized over the sensing sites. In order to have a biochip with a fully scalable number of sensors, a matrix-based biochip was proposed [8]. In this approach, each basic cell comprises a thin film diode (TFD) connected in series with a magnetic tunnel junction (MTJ). The TFDs are used as switching elements while the MTJ is the chosen magnetoresistive sensor, detecting the fringe field of immobilized magnetic markers.

Two TFD types (PIN and Schottky barrier type) were chosen from the technology available in our lab. Fig. 1 shows that the Schottky diodes have a maximum forward bias current at lower voltages than the PIN diodes. However, if this voltage surpasses 1 V, the Schottky diode may be irreversibly damaged. This threshold occurs at 3 V for PIN diodes. The higher conductance of the PIN diodes has an immediate impact in allowing diode size reduction, and/or using MTJs with lower resistance and larger area resulting in an increased dynamic range of the sensor (number of beads detected). The PIN diodes also show a higher ON/OFF ratio (10^8 for PIN vs 10^6 for Schottky TFD) which means that a matrix with more elements can be developed. Furthermore, a higher process yield was found when compared with Schottky diodes.

In order to evaluate the sensitivity of the combined TFD+MTJ device for magnetic label detection, the noise level of the diode-MTJ series must be analyzed. In the typical

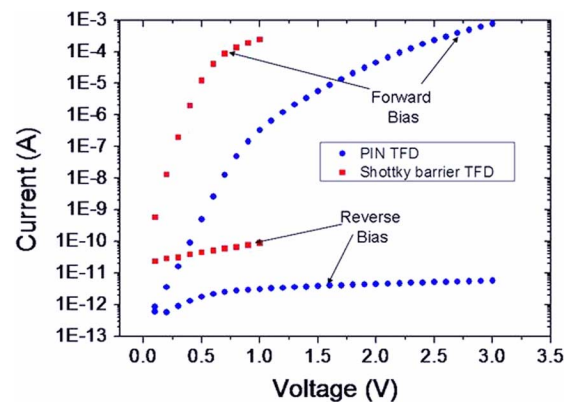


Fig. 1. $200 \times 200 \mu\text{m}^2$ PIN and $200 \times 200 \mu\text{m}^2$ Schottky TFD I-V curve.

MR biosensor assay, a low frequency bead magnetizing field is used (few Hz to few kHz). The excitation frequency should be chosen such as the $1/f$ noise contribution is strongly reduced (meaning working near the thermal background limit). The major goal of this work is to quantify the extra noise coming from the TFD at each matrix site (as compared to a MTJ sensor alone), and to determine the minimum number of particle markers that can be detected for a certain excitation frequency and sensor layout.

II. EXPERIMENTAL METHOD

Fig. 2 shows the schematic cross section of the fabricated TFD-MTJ matrix cell, where the diode (PIN or Schottky) is next to the MTJ. The MTJ was first deposited on top of a glass substrate using an ion beam Nordiko 3000 system with the following structure: Ta 90 Å/Ni₈₀Fe₂₀ 70 Å/Mn₇₆Ir₂₄ 250 Å/(Co₈₀Fe₂₀)₉₀B₁₀ 50 Å/Al 9 Å(+oxidation)/(Co₈₀Fe₂₀)₉₀B₁₀ 50 Å/Ni₈₀Fe₂₀ 70 Å/Ta 60 Å/Ti₁₀W₉₀(N) 150 Å (details on MTJ fabrication are given in [9]). A field of 40 Oe was used during the deposition of the magnetic layers (crossed anisotropies). The aluminum

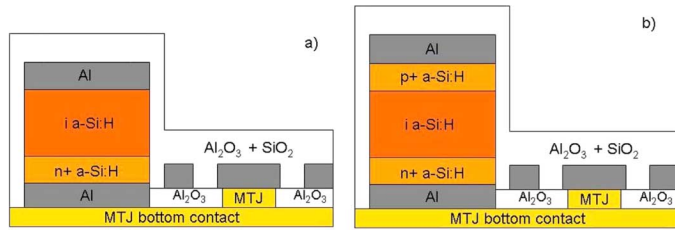


Fig. 2. (a) Film stack of a matrix element composed by a MTJ and a a-Si:H Schottky diode. (b) Film stack of a matrix element composed by a MTJ and a a-Si:H PIN diode.

TABLE I

MAGNETIC MOMENT UNDER A 15 Oe MAGNETIC FIELD, AVERAGE SUSCEPTIBILITY IN THE 0 TO 40 Oe FIELD RANGE AND AVERAGE MAGNETIC FIELD $\langle H_p \rangle$ OVER THE SENSING AREA OF ONE PARTICLE ABOVE THE CENTER OF THE SENSOR AT A DISTANCE OF 0.6 μm FOR DIFFERENT NANO-SIZED SUPERPARAMAGNETIC PARTICLES [1]

Diameter (nm)	Susceptibility (emu/Oe)	Moment under 15 Oe field (emu)	$\langle H_p \rangle$ on a $2 \times 10 \mu\text{m}^2$ sensor area (Oe)
250	3.1×10^{-15}	1.6×10^{-13}	1.7×10^{-2}
130	4.1×10^{-16}	2.0×10^{-14}	2.7×10^{-3}
100	1.2×10^{-17}	1.8×10^{-16}	2.5×10^{-5}
50	3.7×10^{-18}	5.6×10^{-17}	7.8×10^{-6}

oxide tunneling barrier was obtained by remote plasma oxidation [9]. After patterning (by ion milling) down to $2 \times 10 \mu\text{m}^2$ and isolating the MTJ electrodes with a RF sputtered 500 Å thick Al₂O₃ layer, a 2000 Å thick Al film (AlSi_{1%}Cu_{0.5%}) capped by a 150 Å thick Ti₁₀W₉₀(N) layer was deposited by magnetron sputtering. This layer was patterned by ion milling (to remove TiW layer) and Al wet etching to form the diode bottom contact, the matrix columns, and the U-shaped particle focusing lines [12]. The hydrogenated amorphous silicon (a-Si:H) diode stacks, 200 Å+na-Si:H/2000 Å intrinsic a-Si:H (for Schottky diodes) or 200 Å n+- a-Si:H/5000 Å intrinsic a-Si:H/200 Å p+- a-Si:H (for PIN diodes) were then deposited by RF plasma enhanced chemical vapor deposition [10]. After patterning the diodes down to $200 \times 200 \mu\text{m}^2$ [Fig. 2(a) and (b)] using reactive ion etch and isolating the column lines with a 2500 Å thick layer of Al₂O₃, a 3000 Å Al/150 Å TiW(N) metallic layer deposited and patterned, forming the lines of the matrix. Afterwards, a 1000 Å thick Al₂O₃ and a 2000 Å thick SiO₂ layer were deposited to provide a suitable surface for biomolecule immobilization and to protect the chip from corrosion during chemical and biological assays. Finally, a 280 °C annealing under a 1 Tesla field in the MTJ pinned layer direction was done.

The noise of the TFD and the MTJ structures was measured using a low-noise amplifier Stanford Research System (SRS) SIM910 and a real-time spectrum analyzer with 2 Hz bandwidth in the DC to 1 kHz frequency range to respectively amplify and measure the noise spectrum [11].

The superparamagnetic particles used for device characterization are composed of magnetite (75% for Nanomag-D and 35% for Nanomag-D-spio) dispersed in a dextran matrix (Micromod, Germany) and have a diameter of 250 nm (Nanomag-D), 130 nm (Nanomag-D), 100 nm (Nanomag-D-spio), and 50 nm (Nanomag-D-spio) (see Table I for the magnetic characteristics).

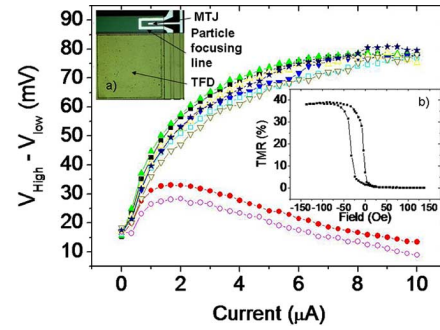


Fig. 3. Maximum voltage change in the MTJ-diode device (when the MTJ is switched from the parallel to antiparallel state) as a function of the applied current on each elements of a 3×3 matrix. Inset: (a) Top view of a matrix element composed by a TFD and a MTJ. A U-shaped focusing line can be used to focus magnetic particles over the sensor [12]. (b) Transfer curve of a MTJ with a resistance of 30 k Ω and an area of $2 \times 10 \mu\text{m}^2$.

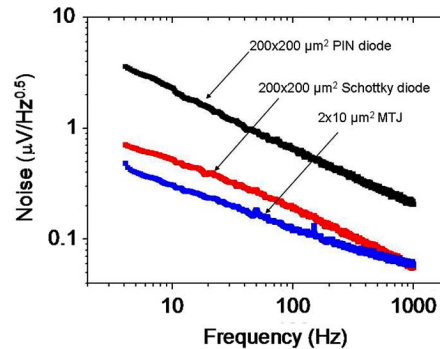


Fig. 4. Noise spectra at a 15 Oe field of a 30 k Ω MTJ with a Hooge constant of $5 \times 10^{-9} \mu\text{m}^2$ and an area of $2 \times 10 \mu\text{m}^2$, and of a $200 \times 200 \mu\text{m}^2$ PIN and Schottky TFD.

III. EXPERIMENTAL RESULTS AND DISCUSSION

The I - V curves of the fabricated TFD (Schottky and PIN) and the transfer curves of the fabricated MTJ are shown in Figs. 1 and 3 (inset), respectively. The MTJs shows a tunneling magnetoresistance ratio (TMR) of 40% and a resistance of 30 k Ω .

A 3×3 cell matrix with PIN TFDs in series with MTJs as the basic cell element [Fig 3(a)] was measured. Fig. 3 shows the voltage change (ΔV) obtained from the MTJ-TFD series, as the MTJ is switched from the parallel to antiparallel resistance states, as a function of the biasing current. Due to the TMR decrease upon bias voltage increase, a ΔV peak is observed at a certain biasing current as described in [8]. This peak depends on the MTJ resistance and TMR [8]. In the presented 3×3 matrix (Fig. 3), 7 MTJs show this peak at the 10 μA (normally working MTJ) while two of them had a deficient MTJ showing lower TMR and higher resistance.

Fig. 4 shows the measured noise spectrum of a 5.7 μA biased MTJ (at 0 Oe field), 4.4 μA biased $200 \times 200 \mu\text{m}^2$ PIN TFD, and a 5.3 μA biased $200 \times 200 \mu\text{m}^2$ Schottky TFD. In the DC to 1 kHz frequency range both devices (MTJ and TFD) are still in the $1/f$ dominated noise region. Both TFDs showed higher noise than the MTJ. The $200 \times 200 \mu\text{m}^2$ PIN diodes have a substantially higher noise level when compared with Schottky diodes despite being more suitable for matrix applications.

From the noise level measured in each device, one can now predict the minimum number of particles that the matrix cells

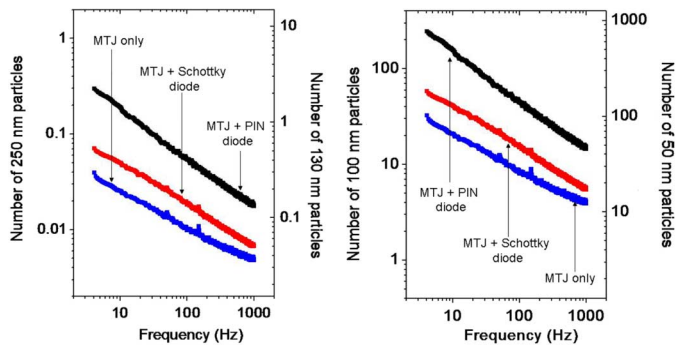


Fig. 5. Simulated minimum number of 250, 130, 100, and 50 nm particles that a MTJ, a MTJ + Schottky diode, and a MTJ + PIN diode device allows to detect.

can measure. The noise spectral density of the MTJ, MTJ+PIN diode, and MTJ+Schottky diode was converted into voltage at each measurement frequency (1 Hz bandwidth assumed) and then into equivalent magnetic field using the MTJ sensitivity of 0.6 mV/Oe. The number of particles required to generate the calculated field was obtained from the individual field of each particle. This field was averaged over the MTJ area ($2 \times 10 \mu\text{m}^2$) and calculated assuming the particle placed at a distance of 0.6 μm (which corresponds to the thickness of the metallic top contact+passivation layer) above the center of the sensor with an in-plane 15 Oe (peak to peak) ac magnetizing field. It was assumed that there is no mutual interaction between beads since what is required is to determine if single particle detection is achievable. Fig. 5 shows the calculated number of particles that each device (stand alone MTJ, MTJ+PIN diode, or MTJ+Schottky diode) was able to detect. These calculations should be taken only as valid in the limit of small number of particles.

At 30 Hz both devices can measure a single 250 nm particle. For the 130 nm particles, only the MTJ+PIN diode device is not able to detect a single particle for frequencies below 30 Hz. The 100 nm and 50 nm particles have a lower magnetic moment than the previous ones and none of the devices can detect a single particle in the DC to 1 kHz range. The standalone MTJ is the device that can detect the lower number of particles (more than ten 50 nm-sized particles and four 100 nm-sized particles) as expected from its lower noise level. The Schottky barrier TFD+MTJ configuration is the second most sensitive device, being able to detect down to seven 100 nm-sized particles and twenty 50 nm-sized particles (at 1 kHz), while at the same frequency the MTJ+PIN diode can only detect 3 times more 100 nm particles (5 times with 50 nm). From the point of

view of noise, the matrix-based biochips using a PIN diode as switching element show lower particle sensitivity than the ones using Schottky barrier TFDs. Nevertheless, if a proper detection frequency is used, at best less than one hundred of the smallest 50 nm particles can be detected by a matrix-based system.

IV. CONCLUSION

In this paper, a working 3×3 cell matrix was presented and the noise of the different devices (TFDs, PIN and Schottky, and MTJs) comprised in this matrix was studied. Simulations of the magnetic field created by superparamagnetic nanoparticles show the possibility of detecting single 250 nm and 130 nm particles, and about twenty 50 nm particles (at 1 kHz).

ACKNOWLEDGMENT

This work was supported by the portuguese national project POSC/EEA-ESE/58523/2004 and POCTI/CTM/59411/2004, and the european projects EC FP6 under the contracts NMP4-CT-2005-016833 (SNIP2CHIP) and NMP4-CT-2005-017210 (Biomagsense). F. A. Cardoso and R. Ferreira are grateful to FCT for the grant SFRH/BD/23756/2005 and SFRH/BD/6501/2001.

REFERENCES

- [1] P. P. Freitas, H. A. Ferreira, D. L. Graham, L. A. Clarke, M. D. Amaral, V. Martins, L. Fonseca, and J. M. S. Cabral, *Magnetolectronics*, M. Johnson, Ed. New York: Academic Press, 2004.
- [2] D. L. Graham, H. A. Ferreira, and P. P. Freitas, *Trends Biotechnol.*, vol. 22, p. 455, 2004.
- [3] J. C. Rife, M. M. Miller, P. E. Sheehan, C. R. Tamaña, M. Tondra, and L. J. Whitman, *Sens. Actuators A*, vol. 107, p. 209, 2003.
- [4] J. Schotter, P. B. Kamp, A. Becker, A. Pühler, G. Reiss, and H. Brückl, *Biosens. Bioelect.*, vol. 19, p. 1149, 2004.
- [5] H. A. Ferreira, D. L. Graham, N. Feliciano, L. A. Clarke, M. D. Amaral, and P. P. Freitas, *IEEE Trans. Magn.*, vol. 41, pp. 4140–4142, 2005.
- [6] W. Shen, X. Liu, D. Mazumdar, and G. Xiao, *Appl. Phys. Lett.*, vol. 86, p. 253901, 2005.
- [7] L. Ejsing, M. F. Hansen, A. K. Menon, H. A. Ferreira, D. L. Graham, and P. P. Freitas, *Appl. Phys. Lett.*, vol. 84, pp. 4729–0, 2004.
- [8] F. A. Cardoso, H. A. Ferreira, J. P. Conde, V. Chu, P. P. Freitas, D. Vidal, J. Germano, L. Sousa, M. S. Piedade, B. Andrade, and J. M. Lemos, *J. Appl. Phys.*, vol. 99, p. 08B307, 2006.
- [9] S. Cardoso, V. Gehanno, R. Ferreira, and P. P. Freitas, *IEEE Trans. Magn.*, vol. 35, p. 2952, 1999.
- [10] R. C. Sousa, P. P. Freitas, V. Chu, and J. P. Conde, *IEEE Trans. Magn.*, vol. 35, p. 2832, 1999.
- [11] R. Ferreira, P. P. Freitas, J. Langer, B. Ocker, and W. Maass, *J. Appl. Phys.*, vol. 99, p. 08K706, 2006.
- [12] H. A. Ferreira, N. Feliciano, D. L. Graham, L. A. Clarke, M. D. Amaral, and P. P. Freitas, *Appl. Phys. Lett.*, vol. 87, p. 013901, 2005.